ACS OMEGA

Article

Cite This: ACS Omega 2018, 3, 8589−8594

http://pubs.acs.org/journal/acsodf

Zirconyl Clindamycinphosphate Antibiotic Nanocarriers for Targeting Intracellular Persisting *Staphylococcus aureus*

Joachim G. Heck,[†] Katharina Rox,[‡,§] Heinrich Lünsdorf,[‡] Thorsten Lückerath,[†] Nicole Klaassen,[†] Eva Medina,[‡] Oliver Goldmann,*[,‡] and Claus Feldmann*[,†]

[†]Institute of Inorganic Chemistry, Karlsruhe Institute of Technology (KIT), Engesserstrasse 15, 76131 Karlsruhe, Germany

[‡]Helmholtz-Zentrum für Infektionsforschung, Inhoffenstrasse 7, D-38124 Braunschweig, Germany

[§]Deutsches Zentrum für Infektionsforschung, Partner Site Hannover-Braunschweig, Inhoffenstrasse 7, D-38124 Braunschweig, Germany

Supporting Information

ABSTRACT: $[ZrO]^{2+}[CLP]^{2-}$ (CLP: clindamycinphosphate) inorganic−organic hybrid nanoparticles (IOH-NPs) represent a novel strategy to treat persisting, recurrent infections with multiresistant *Staphylococcus aureus*. $[ZrO]^{2+}[CLP]^{2-}$ is prepared in water and contains the approved antibiotic with unprecedented high load (82 wt % CLP per nanoparticle). The IOH-NPs result in 70−150-times higher antibiotic concentrations at difficult-to-reach infection sites, offering new options for improved drug delivery for chronic and difficult-to-treat infections.

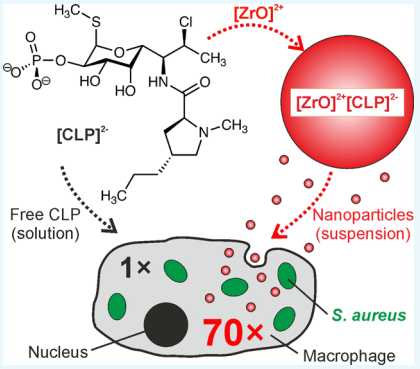

1. INTRODUCTION

The overuse and inappropriate application of antibiotics is well known to lead to the emergence of antibiotic resistance—and even more challenging—to an increase of multidrug resistances (MDR) among several bacterial species.[1] MDR *Mycobacterium tuberculosis*, or Gram-negative bacteria with extended-spectrum *β*-lactamase production (e.g., *Klebsiella pneumoniae*, *Pseudomonas aeruginosa*, and *Enterobacter* species) and among Gram-positive bacteria, especially *Staphylococcus aureus* (*S. aureus*), have become a major problem for the global healthcare system by increasing healthcare costs due to high morbidity and mortality rates and prolonged hospitalization.[2,3]

A central issue in the development of MDR bacteria is related to the fact that classical treatment strategies often lead to insufficient levels of anti-infectives in various niches of the host such as the intracellular milieu, rendering the treatment less efficient and increasing the threat that pathogens become resistant.[2−6] *S. aureus*, for example, is known to establish intracellular infection reservoirs because of internalization and persistence in several host cells (e.g., mast cells, dendritic cells, macrophages, epithelial cells, and osteoblasts).[3,7−11] Certain *S. aureus* subpopulations (small colony variants) are even well adapted to persist for long periods in the intracellular milieu,[12−15] and they are associated with chronic, relapsing, and therapy-refractory infections such as osteomyelitis or cystic fibrosis.[16−19]

Promising concepts to conquer these problems and to restrict antimicrobial resistance relate to the development of new antimicrobial agents or—equally important—the evolution of more efficient dosage forms of conventional antibiotics for obtaining sufficient concentration levels in the intracellular milieu to guarantee bacterial eradication.[2−6] Typically, the maximum concentration of antibiotics, however, is limited by solubility/availability (in blood, cells, tissue), penetration (through membranes), retention time (due to biodegradation or excretion), as well as by induced side effects. Higher concentrations within the intracellular milieu could be achieved via more efficient uptake into infected cells and tissue. In this regard, several nanoparticle-based concepts were suggested (e.g., tuberculosis treatment)[20,21] that use the different uptake of nanoparticles (i.e., phagocytosis and pinocytosis) in comparison to molecular antibiotics in solution (i.e., via ion channels or passive diffusion through lipid double layers).[22,23]

Nanoparticle-based concepts for antibiotic delivery predominately relate to organic polymers and micelles[24−27] as well as inorganic compounds (e.g., SiO_2, Fe_2O_3, Ag, and Au),[20,21,28−34] in which the antibiotic is encapsulated. These concepts intrinsically have the disadvantage of comparably low drug contents (typically <10 wt %) in mainly nonactive matrices as the majority material. In some cases, moreover, elaborate, multistep synthesis is needed and/or the particle size

Received: April 3, 2018
Accepted: July 13, 2018
Published: August 2, 2018

DOI: 10.1021/acsomega.8b00637
ACS Omega 2018, 3, 8589−8594

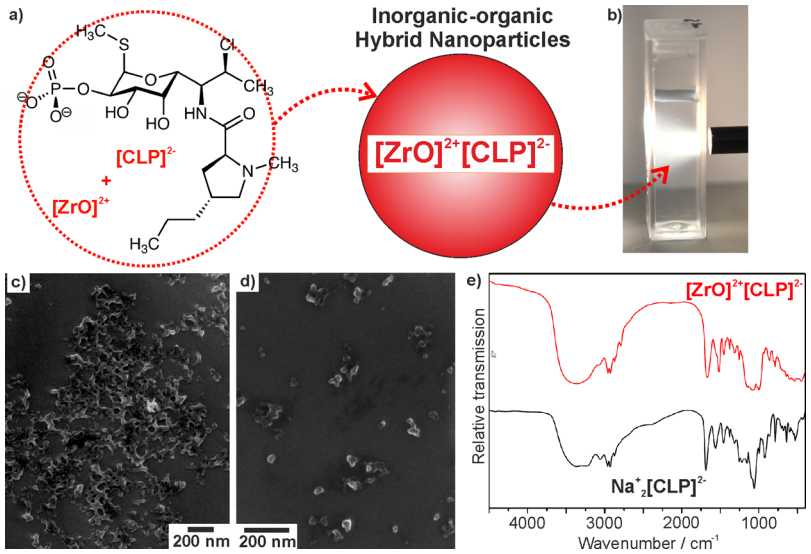

Figure 1. Scheme illustrating the water-based synthesis of $[ZrO]^{2+}[CLP]^{2-}$ IOH-NPs: (a) structure of antibiotic $[CLP]^{2-}$ anion; (b) photograph of aqueous $[ZrO]^{2+}[CLP]^{2-}$ suspension; (c + d) electron microscopy of nanoparticles; and (e) FT-IR spectra [with $Na_2(CLP)$ as reference].

is too large (>150 nm) for what is considered as optimal for biomedical nanoparticle applications (50−100 nm).[20,21,28−34] All in all, nanoparticular antibacterial agents appear to have great potential to revolutionize the diagnosis and treatment of bacterial infections.[35−40]

To address the challenge of intracellular MDR bacteria, we here suggest saline $[ZrO]^{2+}[CLP]^{2-}$ inorganic−organic hybrid nanoparticles (IOH-NPs) as a novel nanocontainer concept to deliver antibiotics with extremely high concentration directly to *S. aureus* in intracellular niches. $[ZrO]^{2+}[CLP]^{2-}$ is an insoluble, saline compound, made in water, which contains an unprecedented high load of 82 wt % of antibiotic $[CLP]^{2-}$ (CLP: clindamycinphosphate). CLP is a clinically approved pro-drug for the active last resort antibiotic clindamycin (CL).[41,42] Both—CLP and CL—are highly bacteriostatic, bactericidal (at higher concentration), and widely used to treat staphylococcal infections—but by now only in dissolved, free form.[41,42]

2. RESULTS AND DISCUSSION

2.1. Material Synthesis and Characterization. $[ZrO]^{2+}[CLP]^{2-}$ was prepared by injecting an aqueous solution of $ZrOCl_2 \times 8H_2O$ to aqueous solutions of $Na_2(CLP)$ at 55 °C (Figure 1a). The synthesis compares to our previously presented concept of phosphate-based IOH-NPs with a general composition $[ZrO]^{2+}[R_{Function}OPO_3]^{2-}$.[43,44] Herein, the inorganic cation $[ZrO]^{2+}$ and a functional organic anion $[R_{Function}OPO_3]^{2-}$ together form a saline hybrid material. $[ZrO]^{2+}$ as the cation and a phosphate group as part of the organic anion guarantee for the insolubility of the IOH-NPs in water (Figure 1a). On the basis of different functional organic anions, a wide range of IOH-NPs entailing various functionalities such as fluorescence, magnetism, or drug delivery can be realized so that the IOH-NPs become suitable for multimodal imaging and/or cancer treatment (Supporting Information: Figure S1).[43,44] Here, we can expand the material concept to antibiotic nanocarriers for the first time. To obtain the saline $[ZrO]^{2+}[CLP]^{2-}$ IOH-NPs and colloidally stable suspensions, particle nucleation and particle growth have to be performed precisely (Figure 1b; Supporting Information).[45] $[ZrO]^{2+}[CLP]^{2-}$ is insoluble in water and can be easily suspended in polar solvents such as water, ethanol, diethylene glycol, or biological buffers (e.g., HEPES and aqueous dextran). Slow dissolution of the $[ZrO]^{2+}[CLP]^{2-}$ IOH-NPs in an active metabolism—similar to CLP as conventional pro-drug in solution—results in the release of CL as the active drug in the presence of phosphatases.[41,42]

On the basis of the good availability of CL as a standard anti-infective and the low-cost aqueous synthesis, $[ZrO]^{2+}[CLP]^{2-}$ IOH-NPs can be obtained in large quantities and concentrated suspensions (up to 20 mg/mL). Scanning electron microscopy (SEM) (Figure 1c,d) confirms the presence of spherical nanoparticles with a mean diameter of 44 ± 11 nm (calculated by statistical evaluation of 100 particles). The hydrodynamic diameter (73(14) nm) obtained via dynamic light scattering is as large as the value obtained by SEM (Supporting Information: Figure S2), which can be ascribed to the high polarity of water and the resulting expanded rigid solvent shell. Moreover, the absence of any specific surface stabilizer on the as-prepared IOH-NPs needs to be taken into account, which facilitates the synthesis and which allows avoiding any eventual toxic effect of a stabilizer. Energy-dispersive X-ray analysis (EDX), Fourier-transform infrared spectroscopy (FT-IR), thermogravimetry (TG), and elemental analysis (EA) validate the chemical composition of $[ZrO]^{2+}[CLP]^{2-}$ as a new compound. EDX and FT-IR qualitatively prove the presence of $[ZrO]^{2+}$ and $[CLP]^{2-}$ (Figure 1e). Quantification via total organics combustion (TG) shows a weight loss of 66% fitting well with the expectation (calcd. 68%) (Supporting Information: Figure S3). EA data of 33.0 wt % C, 5.6 wt % H, 5.6 wt % N, 4.6 wt % S also agree with the expectation (calcd C: 35.0, H: 4.6, N: 5.3, S: 5.3 wt %).

2.2. Biocompatibility and Cell Uptake. Biocompatibility and cell uptake were verified by feeding $[ZrO]^{2+}[CLP]^{2-}$ IOH-NPs to murine bone marrow derived macrophages (BMDMs)—a cell type generally showing high uptake rates of nanoparticles.[45] BMDMs were grown in sterile 4-chamber slides to form confluent cell monolayers and incubated for 6 h in the presence of $[ZrO]^{2+}[CLP]^{2-}$ IOH-NPs. Within this time

DOI: 10.1021/acsomega.8b00637
ACS Omega 2018, 3, 8589−8594

period, numerous $[ZrO]^{2+}[CLP]^{2-}$ IOH-NPs were phagocytosed and appear within primary lysosomes (pLs) either individually or as electron dense clusters (Figure 2a,b: red

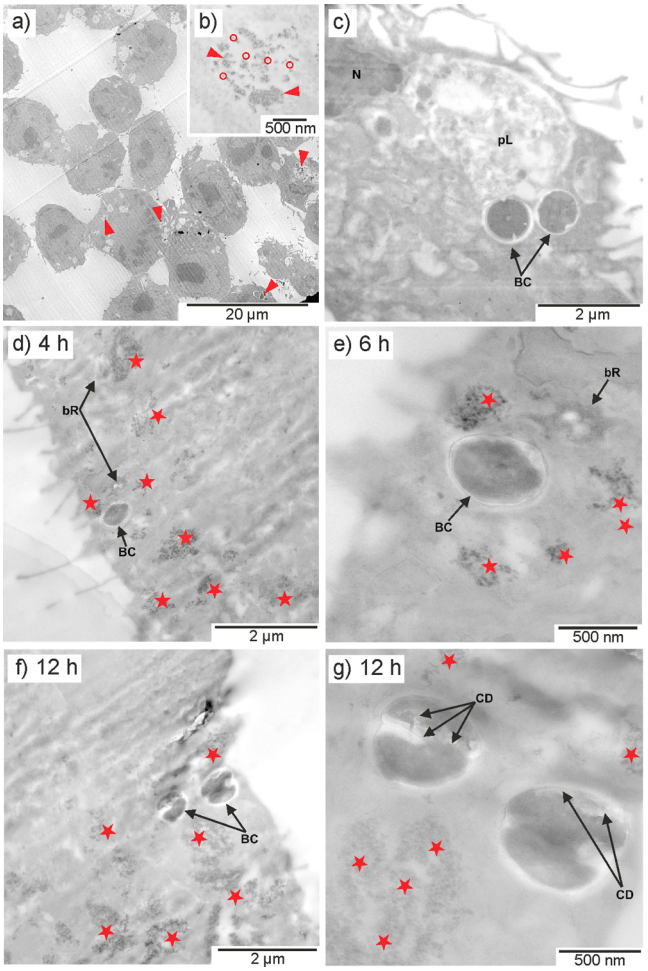

Figure 2. Electron microscopy of murine macrophages, infected with *S. aureus* SH1000 and treated with $[ZrO]^{2+}[CLP]^{2-}$ IOH-NPs: (a) survey of "en face"-sectioned, unstained macrophages, treated with $[ZrO]^{2+}[CLP]^{2-}$ for 6 h (red arrowheads indicate IOH-NP clusters). (b) Detailed view of IOH-NP clusters (red arrowheads) and individual IOH-NPs (red circles) within the pL. (c) Macrophage infected for 12 h with *S. aureus* without IOH-NPs (infection control). (d–g) Macrophages treated with $[ZrO]^{2+}[CLP]^{2-}$ 12 h before infection with *S. aureus* and after 4, 6, and 12 h of incubation (IOH-NP clusters indicated by red stars). Indicators: pL: primary lysosome, N: nucleus, BC: bacterial cell, CD: cellular defects, bR: bacterial remnant.

circles, red arrowheads). *S. aureus* cells are characteristically dispersed within the cytoplasm of infected BMDMs and actively grow within the state of binary fission (Figure 2c). To study the impact of $[ZrO]^{2+}[CLP]^{2-}$ on the viability of intracellular *S. aureus*, infected BMDMs were incubated for 4 h (Figure 2d), 6 h (Figure 2e), and 12 h (Figure 2f,g) with $[ZrO]^{2+}[CLP]^{2-}$ IOH-NPs and examined by electron microscopy. Within BMDMs, individual bacterial cells (BCs) appear surrounded by clusters of $[ZrO]^{2+}[CLP]^{2-}$ within in close distances <500 nm (Figure 2d,g: red stars). After 12 h of incubation with $[ZrO]^{2+}[CLP]^{2-}$ IOH-NPs, the BC shows electron transparencies produced by alterations within the cell wall/subcell wall regions and the plane of binary fission that is associated with an "en-gros" change in cell morphology (Figure 2g). Such cellular defects (CD: black arrows) indicate antibiotic activity and death of the BC.

To validate the presence of $[ZrO]^{2+}[CLP]^{2-}$ IOH-NPs within lysosomes, parallel electron energy-loss spectroscopy and electron spectroscopic imaging (ESI) were performed on unstained 40 nm ultrathin sections of uninfected and *S. aureus*-infected BMDMs incubated with $[ZrO]^{2+}[CLP]^{2-}$ IOH-NPs (Figure 3a,b; Supporting Information: Figure S4). This allows

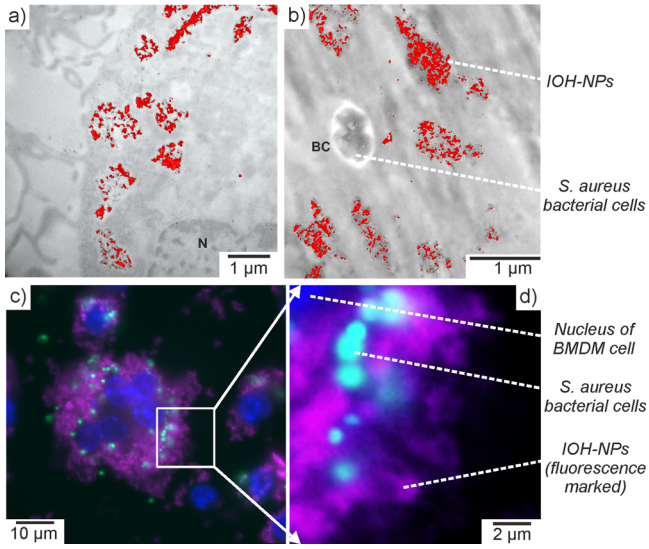

Figure 3. Localization of $[ZrO]^{2+}[CLP]^{2-}$ in BMDM cells: (a) Zr elemental map (Zr-*M45* in red) of macrophage treated for 3 h with $[ZrO]^{2+}[CLP]^{2-}$ IOH-NPs and (b) after infection for 12 h with *S. aureus* and treated for 3 h with $[ZrO]^{2+}[CLP]^{2-}$ IOH-NPs (indicators: BC: bacterial cell, N: nucleus). (c,d) Fluorescence microscopy with $[ZrO]^{2+}[(CLP)_{0.995}(DUT)_{0.005}]^{2-}$ IOH-NPs (purple), *S. aureus* (turquoise), and cellular nuclei (blue, stained with DAPI). Macrophages infected with gfp-expressing *S. aureus* strain SH1000 at an MOI of 10:1 for 1 h followed by co-cultivation with $[ZrO]^{2+}[(CLP)_{0.995}(DUT)_{0.005}]^{2-}$ for 6 h. Enlargement (d) shows co-localization of gfp-expressing *S. aureus* (turquoise) and $[ZrO]^{2+}[(CLP)_{0.995}(DUT)_{0.005}]^{2-}$ IOH-NPs (purple).

discriminating $[ZrO]^{2+}[CLP]^{2-}$ IOH-NPs from other electron dense nanostructures such as ferritins or Fe_2O_3 particles that can be present in BMDMs. Accordingly, Zr-*M45* elemental maps show distinct Zr-*M45* intensities, congruent with $[ZrO]^{2+}[CLP]^{2-}$ clusters of pLs for uninfected (Figure 3a) and *S. aureus*-infected macrophages (Figure 3b), indicating the presence and high load of internalized $[ZrO]^{2+}[CLP]^{2-}$ IOH-NPs. To validate efficient uptake and to ensure the intracellular localization of the IOH-NPs, immunofluorescence microscopy was performed using fluorescence-marked $[ZrO]^{2+}[(CLP)_{0.995}(DUT)_{0.005}]^{2-}$ (DUT: dyomics-647 uridine triphosphate; Supporting Information: Figure S1) and gfp-expressing *S. aureus* bacteria (gfp: green fluorescence protein). Similar to the results of EELS and ESI, the macrophages are highly loaded with fluorescent IOH-NPs, which are found in close proximity to the intracellular bacteria (Figure 3c,d). The data indicate a potential localization of IOH-NPs within primary lysosomal compartments. However, further co-localization studies (e.g., using lysotracker) are needed to gain deeper insights in the molecular and cellular uptake mechanisms of IOH-NPs into the host cells.

DOI: 10.1021/acsomega.8b00637
ACS Omega 2018, 3, 8589−8594

2.3. Antibiotic Effect. Having demonstrated that the $[ZrO]^{2+}[CLP]^{2-}$ IOH-NPs were efficiently internalized by BMDMs, their potential toxic effect on cell viability was assessed by measuring the lactate dehydrogenase (LDH) released into the supernatant by $[ZrO]^{2+}[CLP]^{2-}$-treated BMDMs. Generally, the release of the cytoplasmic enzyme LDH into the culture medium is an indication of plasma membrane disruption and cell damage. However, no significant levels of LDH were observed in the supernatant of $[ZrO]^{2+}[CLP]^{2-}$-treated and untreated BMDMs (Supporting Information: Figure S5). These results clearly indicate a lack of toxicity of $[ZrO]^{2+}[CLP]^{2-}$ IOH-NPs for BMDMs after 24 h of incubation.

To verify if $[ZrO]^{2+}[CLP]^{2-}$ IOH-NPs (in suspension) have an advantage over free CLP (in solution) to kill intracellular *S. aureus*, professional phagocyte BMDMs and nonprofessional phagocytic human epithelial Hep2 cells were infected with the *S. aureus* strain SH1000 at a multiplicity of infection of 10 bacteria per 1 eukaryotic cell for 1 h. The infection was followed by treatment for 2 h with either $[ZrO]^{2+}[CLP]^{2-}$ (suspension) or dissolved CLP [i.e., solution of $Na_2(CLP)$]. Untreated infected cells were used for comparison. Cells were harvested 4 h (nonhatched bars) and 24 h (hatched bars) after infection, washed twice with sterile phosphate-buffered saline, and lysed with ddH_2O for 5 min to release intracellular bacteria. Thereafter, the number of viable intracellular bacteria was counted after platting serial dilutions on blood agar plates. As a result, the number of viable intracellular bacteria is significantly lower in macrophages (Figure 4a) as well as in

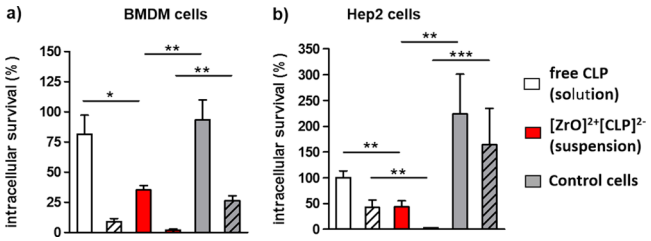

Figure 4. Intracellular survival of *S. aureus* within macrophages (BMDMs) (a) and epithelial Hep2 cells (b) 4 h (nonhatched bars) and 24 h (hatched bars) after infection (cells infected for 1 h with an MOI of 10:1; level of intracellular bacteria 1 h after infection referred to as 100%). Data with mean ± SD of three experiments (***p < 0.0005, **p < 0.005, *p < 0.05).

Hep2 cells (Figure 4b) after treatment with $[ZrO]^{2+}[CLP]^{2-}$ (suspension) compared to untreated cells and cells treated with dissolved CLP (solution). Most remarkably, solutions of free CLP do not show any effect on BMDMs 4 h after infection (Figure 4a), whereas the IOH-NPs significantly reduce the survival rate of intracellular *S. aureus*. In non-phagocytic Hep2 cells, a significant difference between $[ZrO]^{2+}[CLP]^{2-}$ (suspension) and dissolved CLP was also obtained 24 h after infection (Figure 4b), clearly indicating the advantage of the IOH-NP drug delivery concept for cells with low bacterial killing ability. All in all, this clearly demonstrates that CL is significantly more efficient at targeting intracellular *S. aureus* when delivered as $[ZrO]^{2+}[CLP]^{2-}$ IOH-NPs than in the dissolved free form.

To determine if the superior bactericidal efficiency of CL-loaded $[ZrO]^{2+}[CLP]^{2-}$ IOH-NPs over dissolved, free CL is provoked by a more efficient antibiotic penetration and retention in the intracellular milieu, the loading kinetics of either $[ZrO]^{2+}[CLP]^{2-}$ IOH-NPs (suspension) or free CL (solution) into eukaryotic cells was analyzed in BMDMs. Hence, BMDMs were incubated with $[ZrO]^{2+}[CLP]^{2-}$ IOH-NPs, dissolved CLP (Figure 5) and dissolved CL hydro-

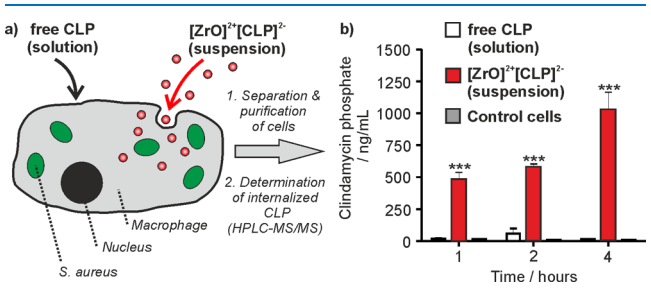

Figure 5. Intracellular CL levels within macrophages 1, 2, and 4 h after co-cultivation with $[ZrO]^{2+}[CLP]^{2-}$ IOH-NPs and dissolved CLP at identical concentrations (50 μg CLP/mL): (a) illustration of uptake and cell treatment; (b) internalized CL after treatment with dissolved CLP (white bars), $[ZrO]^{2+}[CLP]^{2-}$ (red bars), lysates of untreated cells (negative control, gray bars). Data measured by HPLC−MS/MS; mean ± SD of triplicate samples (***p < 0.001).

chloride (CL, Supporting Information: Figure S6) for 1, 2, and 4 h. The amount of intracellular CL was determined in BMDM lysates by high-performance liquid chromatography (HPLC)−mass spectrometry (MS)/MS (Supporting Information) to determine the intracellular CL levels (Figure 5; Supporting Information: Figure S6).

As a result, the internalized CL concentration in macrophages turned out to be 70-times higher after 1 h of incubation when treated with $[ZrO]^{2+}[CLP]^{2-}$ suspensions in comparison to CLP and CL in solution (Figure 5b; Supporting Information: Figure S6, Tables S1, and S2). After 4 h, the internalized CL concentration increases even further and is about 150-times higher after treatment with $[ZrO]^{2+}[CLP]^{2-}$ suspensions (Figure 5b; Supporting Information: Figure S6, Tables S1, and S2). The intracellular levels of CLP reached 1.027 μg per mL in macrophages incubated up to 4 h with the IOH-NPs (suspension). This concentration exceeds the minimal inhibitory concentration of CLP, which was determined as <0.625 μg per mL (Supporting Information: Figure S7). In contrast to the IOH-NP suspensions, the concentration of intracellular CLP after co-cultivation of cells with dissolved CLP remained in the subinhibitory range <0.02 μg per mL. The significantly higher CLP levels reached via the IOH-NP treatment, therefore, is highly promising to address and eventually to solve the challenges related to MDR formation.

The remarkable increase of CLP uptake using IOH-NPs can be attributed to a more efficient uptake of the IOH-NPs by cellular processes such as phago-/pinocytosis and the active acquisition of the IOH-NPs as a phosphate source.[43,44,46,47] These findings coincide with the efficient uptake and the intracellular localization of the $[ZrO]^{2+}[CLP]^{2-}$ IOH-NPs as shown by EELS, ESI (Figure 3a,b), and immunofluorescence microscopy (Figure 3c,d). The uptake of $[ZrO]^{2+}[CLP]^{2-}$ IOH-NPs in BMDMs, finally, shows clear time and concentration dependency (Supporting Information: Figures S8 and S9). The extremely high uptake of $[ZrO]^{2+}[CLP]^{2-}$ by BMDMs can become even more interesting because macrophages can abandon the blood system to attack *S. aureus* at difficult-to-reach niches of the host.[48]

DOI: 10.1021/acsomega.8b00637
ACS Omega 2018, 3, 8589−8594

3. CONCLUSIONS

In sum, $[ZrO]^{2+}[CLP]^{2-}$ IOH-NPs represent a novel nanoparticle-based strategy to treat persisting and recurrent *S. aureus*-caused infections. $[ZrO]^{2+}[CLP]^{2-}$ contains an unprecedented high amount (82 wt %) of clinically approved CLP and shows high uptake at low toxicity. Most interestingly, the IOH-NP suspensions allow 70−150-times higher drug concentration (after 1−4 h of incubation) than the free drug in solution at difficult-to-reach intracellular infection sites. This offers unique options for improved drug delivery to eradicate intracellular bacterial reservoirs during chronic and difficult-to-treat infections. Because macrophages are not limited to the blood system, they can—after loading with $[ZrO]^{2+}[CLP]^{2-}$ IOH-NPs—also attack multiresistant bacteria in various difficult-to-reach niches of the host with the anti-infective in very high concentrations. In principle, the material concept and delivery strategy can be also transferred to other antibiotics as well as to treat other multiresistant bacteria including the relevant species of *Klebsiella*, *Pseudomonas*, or *Enterobacter*.

4. EXPERIMENTAL SECTION

4.1. Synthesis of $[ZrO]^{2+}[CLP]^{2-}$ IOH-NPs. $Na_2(CLP)$ (25 mg, Aldrich, 95.7%) was dissolved in water (50 mL). The pH of this solution was adjusted to 7.0 upon the addition of diluted NaOH (140 μL, 0.5 M). Thereafter, an aqueous solution (5 mL) of $ZrOCl_2 \times 8H_2O$ (4.25 mg, Aldrich, 99%) was injected. After 2 min of intense stirring, the nanoparticles were separated via centrifugation (25 000 rpm, 15 min). To remove all remaining salts, the colorless $[ZrO]^{2+}[CLP]^{2-}$ was resuspended in and centrifuged from H_2O three times. Subsequent to redispersion, highly stable colloidal suspension in water can be obtained (Figure 1b).

■ ASSOCIATED CONTENT

Supporting Information

The Supporting Information is available free of charge on the ACS Publications website at DOI: 10.1021/acsomega.8b00637.

Details regarding analytical techniques for material characterization, synthesis of $[ZrO]^{2+}[CLP]^{2-}$ and fluorescence-marked $[ZrO]^{2+}[(CLP)_{0.95}(DUT)_{0.05}]^{2-}$ IOH-NPs, material characterization, and biological studies (PDF)

■ AUTHOR INFORMATION

Corresponding Authors

*E-mail: oliver.goldmann@helmholtz-hzi.de (O.G.).
*E-mail: claus.feldmann@kit.edu (C.F.)

ORCID

Claus Feldmann: 0000-0003-2426-9461

Notes

The authors declare no competing financial interest.

■ ACKNOWLEDGMENTS

J.G.H. and C.F. thank the Deutsche Forschungsgemeinschaft (DFG) for funding of equipment. K.R. and O.G. thank Sabine Lehne and Janine Schreiber for excellent technical assistance.

■ REFERENCES

(1) World Health Organization (WHO). *Global Health Report*, 2016, ISBN 978 92 4 156480 9.
(2) Fisher, R. A.; Gollan, B.; Helaine, S. Persistent bacterial infections and persister cells. *Nat. Rev. Microbiol.* **2017**, *15*, 453−464.
(3) Medina, E.; Pieper, D. H. Tackling Threats and Future Problems of Multidrug-Resistant Bacteria. *How to Overcome the Antibiotic Crisis*; Current Topics in Microbiology and Immunology; Springer, 2016; Vol. *398*, pp 3−33.
(4) Chellat, M. F.; Raguž, L.; Riedl, R. Targeting Antibiotic Resistance. *Angew. Chem., Int. Ed.* **2016**, *55*, 6600−6626.
(5) Tong, S. Y. C.; Davis, J. S.; Eichenberger, E.; Holland, T. L.; Fowler, V. G. Staphylococcus aureus Infections: Epidemiology, Pathophysiology, Clinical Manifestations, and Management. *Clin. Microbiol. Rev.* **2015**, *28*, 603−661.
(6) Foster, T. J.; Geoghegan, J. A.; Ganesh, V. K.; Höök, M. Adhesion, invasion and evasion: the many functions of the surface proteins of Staphylococcus aureus. *Nat. Rev. Microbiol.* **2014**, *12*, 49−62.
(7) Abel, J.; Goldmann, O.; Ziegler, C.; Höltje, C.; Smeltzer, M. S.; Cheung, A. L.; Bruhn, D.; Rohde, M.; Medina, E. *Staphylococcus aureus* Evades the Extracellular Antimicrobial Activity of Mast Cells by Promoting Its Own Uptake. *J. Innate Immun.* **2011**, *3*, 495−507.
(8) Schindler, D.; Gutierrez, M. G.; Beineke, A.; Rauter, Y.; Rohde, M.; Foster, S.; Goldmann, O.; Medina, E. Dendritic Cells Are Central Coordinators of the Host Immune Response to Staphylococcus aureus Bloodstream Infection. *Am. J. Pathol.* **2012**, *181*, 1327−1337.
(9) Surewaard, B. G. J.; Deniset, J. F.; Zemp, F. J.; Amrein, M.; Otto, M.; Conly, J.; Omri, A.; Yates, R. M.; Kubes, P. Identification and Treatment of the *Staphylococcus aureus* Reservoir in vivo. *J. Exp. Med.* **2016**, *213*, 1141−1151.
(10) Löffler, B.; Tuchscherr, L.; Niemann, S.; Peters, G. Staphylococcus aureus Persistence in Non-professional Phagocytes. *Int. J. Med. Microbiol.* **2014**, *304*, 170−176.
(11) Goldmann, O.; Tuchscherr, L.; Rohde, M.; Medina, E. α-Hemolysin Enhances *Staphylococcus aureus* Internalization and Survival Within Mast Cells by Modulating the Expression of β1 Integrin. *Cell. Microbiol.* **2016**, *18*, 807−819.
(12) Balwit, J. M.; Langevelde, P. V.; Vann, J. M.; Proctor, R. A. Gentamicin-Resistant Menadione and Hemin Auxotrophic Staphylococcus aureus Persist within Cultured Endothelial Cells. *J. Infect. Dis.* **1994**, *170*, 1033−1037.
(13) Grosz, M.; Kolter, J.; Paprotka, K.; Winkler, A.-C.; Schäfer, D.; Chatterjee, S. S.; Geiger, T.; Wolz, C.; Ohlsen, K.; Otto, M.; Rudel, T.; Sinha, B.; Fraunholz, M. Cytoplasmic Replication of *Staphylococcus aureus* upon Phagosomal Escape Triggered by Phenol-soluble Modulin α. *Cell. Microbiol.* **2014**, *16*, 451−465.
(14) Fraunholz, M.; Sinha, B. Intracellular Staphylococcus aureus: Live-in and Let Die. *Front. Cell. Infect. Microbiol.* **2012**, *2*, 43.
(15) Sinha, B.; Fraunholz, M. Staphylococcus aureus Host Cell Invasion and Post-invasion Events. *Int. J. Med. Microbiol.* **2010**, *300*, 170−175.
(16) Proctor, R. A.; von Eiff, C.; Kahl, B. C.; Becker, K.; McNamara, P.; Herrmann, M.; Peters, G. Small Colony Variants: a Pathogenic form of Bacteria that Facilitates Persistent and Recurrent Infections (Review). *Nat. Rev. Microbiol.* **2006**, *4*, 295−305.
(17) Sendi, P.; Rohrbach, M.; Graber, P.; Frei, R.; Ochsner, P. E.; Zimmerli, W. Staphylococcus aureus Small Colony Variants in Prosthetic Joint Infection. *Clin. Infect. Dis.* **2006**, *43*, 961−967.
(18) Kahl, B.; Herrmann, M.; Everding, A. S.; Koch, H. G.; Becker, K.; Harms, E.; Proctor, R. A.; Peters, G. Persistent Infection with Small Colony Variant Strains of Staphylococcus aureus in Patients with Cystic Fibrosis. *J. Infect. Dis.* **1998**, *177*, 1023−1029.
(19) Tuchscherr, L.; Heitmann, V.; Hussain, M.; Viemann, D.; Roth, J.; von Eiff, C.; Peters, G.; Becker, K.; Löffler, B. Staphylococcus aureus Small-Colony Variants are Adapted Phenotypes for Intracellular Persistence. *J. Infect. Dis.* **2010**, *202*, 1031−1040.
(20) Herman, A.; Herman, A. P. Nanoparticles as Antimicrobial Agents: Their Toxicity and Mechanisms of Action. *J. Nanosci. Nanotechnol.* **2014**, *14*, 946−957.
(21) Leidinger, P.; Treptow, J.; Hagens, K.; Eich, J.; Zehethofer, N.; Schwudke, D.; Oehlmann, W.; Lünsdorf, H.; Goldmann, O.; Schaible,

DOI: 10.1021/acsomega.8b00637
ACS Omega 2018, 3, 8589−8594

U. E.; Dittmar, K. E.; Feldmann, C. Isoniazid@Fe2O3 Nanocontainers and Their Antibacterial Effect on Tuberculosis Mycobacteria. *Angew. Chem., Int. Ed.* **2015**, *54*, 12597−12601.
(22) Kafshgari, M. H.; Harding, F. J.; Voelcker, N. H. Insights into Cellular Uptake of Nanoparticles (Review). *Curr. Drug Delivery* **2015**, *12*, 63−77.
(23) Ding, H.-M.; Ma, Y.-Q. Theoretical and Computational Investigations of Nanoparticle-Biomembrane Interactions in Cellular Delivery (Review). *Small* **2015**, *11*, 1055−1071.
(24) Liu, Y.; van der Mei, H. C.; Zhao, B.; Zhai, Y.; Cheng, T.; Li, Y.; Zhang, Z.; Busscher, H. J.; Ren, Y.; Shi, L. Eradication of Multidrug-Resistant Staphylococcal Infections by Light-Activatable Micellar Nanocarriers in a Murine Model. *Adv. Funct. Mater.* **2017**, *27*, 1701974.
(25) Thiyagarajan, D.; Das, G.; Ramesh, A. Amphiphilic Cargo-loaded Nanocarrier Enhances Antibiotic Uptake and Perturbs Efflux: Effective Synergy for Mitigation of Methicillin-resistant Staphylococcus aureus. *ChemMedChem* **2017**, *12*, 1125−1132.
(26) Takahashi, C.; Saito, S.; Suda, A.; Ogawa, N.; Kawashima, Y.; Yamamoto, H. Antibacterial activities of polymeric poly(DL-lactide-co-glycolide) Nanoparticles and Soluplus Micelles Against Staphylococcus Epidermidis Biofilm and Their Characterization. *RSC Adv.* **2015**, *5*, 71709−71717.
(27) Díez-Martínez, R.; García-Fernández, E.; Manzano, M.; Martínez, Á.; Domenech, M.; Vallet-Regí, M.; García, P. Auranofin-loaded Nanoparticles as a New Therapeutic Tool to Fight Streptococcal Infections. *Sci. Rep.* **2016**, *6*, 19525.
(28) Kwon, E. J.; Skalak, M.; Bertucci, A.; Braun, G.; Ricci, F.; Ruoslahti, E.; Sailor, M. J.; Bhatia, S. N. Porous Silicon Nanoparticle Delivery of Tandem Peptide Anti-infectives for the Treatment of Pseudomonas aeruginosa Lung Infections. *Adv. Mater.* **2017**, *29*, 1701527.
(29) Geilich, B. M.; Gelfat, I.; Sridhar, S.; van de Ven, A. L.; Webster, T. J. Superparamagnetic Iron Oxide-encapsulating Polymersome Nanocarriers for Biofilm Eradication. *Biomaterials* **2017**, *119*, 78−85.
(30) Ruehle, B.; Clemens, D. L.; Lee, B.-Y.; Horwitz, M. A.; Zink, J. I. A Pathogen-Specific Cargo Delivery Platform Based on Mesoporous Silica Nanoparticles. *J. Am. Chem. Soc.* **2017**, *139*, 6663−6668.
(31) Qadri, S.; Haik, Y.; Mensah-Brown, E.; Bashir, G.; Fernandez-Cabezudo, M. J.; al-Ramadi, B. K. Metallic Nanoparticles to Eradicate Bacterial Bone Infection. *Nanomedicine* **2017**, *13*, 2241−2250.
(32) Thirumurugan, G.; Seshagiri Rao, J. V. L. N.; Dhanaraju, M. D. Elucidating Pharmacodynamic Interaction of Silver Nanoparticle - Topical Deliverable Antibiotics. *Sci. Rep.* **2016**, *6*, 29982.
(33) Kim, T.; Braun, G. B.; She, Z.-g.; Hussain, S.; Ruoslahti, E.; Sailor, M. J. Composite Porous Silicon-Silver Nanoparticles as Theranostic Antibacterial Agents. *ACS Appl. Mater. Interfaces* **2016**, *8*, 30449−30457.
(34) Wang, Y.; Wan, J.; Miron, R. J.; Zhao, Y.; Zhang, Y. Antibacterial Properties and Mechanisms of Gold-silver Nanocages. *Nanoscale* **2016**, *8*, 11143−11152.
(35) Li, L.-L.; Wang, H. Infection-targeted bactericidal nanoparticles. *Nat. Biomed. Eng.* **2018**, *2*, 56−57.
(36) Hussain, S.; Joo, J.; Kang, J.; Kim, B.; Braun, G. B.; She, Z.-G.; Kim, D.; Mann, A. P.; Mölder, T.; Teesalu, T.; Carnazza, S.; Guglielmino, S.; Sailor, M. J.; Ruoslahti, E. Antibiotic-loaded Nanoparticles Targeted to the Site of Infection Enhance Antibacterial Efficacy (Review). *Nat. Biomed. Eng.* **2018**, *2*, 95−103.
(37) Zaidi, S.; Misba, L.; Khan, A. U. Nano-therapeutics: A Revolution in Infection Control in Post Antibiotic Era (Review). *Nanomedicine* **2017**, *13*, 2281−2301.
(38) Hammond, P. T. Nano Tools Pave the Way to New Solutions in Infectious Disease. *ACS Infect. Dis.* **2017**, *3*, 554−558.
(39) Zazo, H.; Colino, C. I.; Lanao, J. M. Current Applications of Nanoparticles in Infectious Diseases (Review). *J. Controlled Release* **2016**, *224*, 86−102.
(40) Miller, K. P.; Wang, L.; Benicewicz, B. C.; Decho, A. W. Inorganic Nanoparticles Engineered to Attack Bacteria (Review). *Chem. Soc. Rev.* **2015**, *44*, 7787−7807.
(41) Azeh, I.; Gerber, J.; Wellmer, A.; Wellhausen, M.; Koenig, B.; Eiffert, H.; Nau, R. Protein Synthesis Inhibiting Clindamycin Improves Outcome in a Mouse Model of *Staphylococcus aureus* Sepsis Compared with the Cell Wall Active Ceftriaxone. *Crit. Care Med.* **2002**, *30*, 1560−1564.
(42) Reeves, D. S.; Holt, H. A.; Phillips, I.; King, A.; Miles, R. S.; Paton, R.; Wise, R.; Andrews, J. M. Activity of Clindamycin Against *Staphylococcus aureus* and Staphylococcus epidermidis from four UK Centres. *J. Antimicrob. Chemother.* **1991**, *27*, 469−474.
(43) Heck, J. G.; Napp, J.; Simonato, S.; Möllmer, J.; Lange, M.; Reichardt, H. R.; Staudt, R.; Alves, F.; Feldmann, C. Multifunctional Phosphate-based Inorganic-Organic Hybrid Nanoparticles. *J. Am. Chem. Soc.* **2015**, *137*, 7329−7336.
(44) Poß, M.; Tower, R. J.; Napp, J.; Appold, L. C.; Lammers, T.; Alves, F.; Glüer, C.-C.; Boretius, S.; Feldmann, C. Multimodal $[GdO]^{+}[ICG]^{-}$ Nanoparticles for Optical, Photoacoustic, and Magnetic Resonance Imaging. *Chem. Mater.* **2017**, *29*, 3547−3554.
(45) Gottstein, C.; Wu, G.; Wong, B. J.; Zasadzinski, J. A. Precise Quantification of Nanoparticle Internalization. *ACS Nano* **2013**, *7*, 4933−4945.
(46) Zhang, S.; Gao, H.; Bao, B. Physical Principles of Nanoparticle Cellular Endocytosis (Review). *ACS Nano* **2015**, *9*, 8655−8671.
(47) Ding, H. M.; Ma, Y.-Q. Theoretical and Computational Investigations of Nanoparticle−Biomembrane Interactions in Cellular Delivery (Review). *Small* **2015**, *11*, 1055−1071.
(48) Miller, M. A.; Zheng, Y.-R.; Gadde, S.; Pfirschke, C.; Zope, H.; Engblom, C.; Kohler, R. H.; Iwamoto, Y.; Yang, K. S.; Askevold, B.; Kolishetti, N.; Pittet, M.; Lippard, S. J.; Farokhzad, O. C.; Weissleder, R. Tumour-associated Macrophages Act as a Slow-release Reservoir of Nano-therapeutic Pt(IV) Pro-drug. *Nat. Commun.* **2015**, *6*, 8692.

DOI: 10.1021/acsomega.8b00637
ACS Omega 2018, 3, 8589−8594